HHS Public Access

Author manuscript

Mol Cell. Author manuscript; available in PMC 2016 March 19.

Published in final edited form as:

Mol Cell. 2015 March 19; 57(6): 1099–1109. doi:10.1016/j.molcel.2015.01.035.

The ubiquitous *yybP-ykoY* riboswitch is a manganese-responsive regulatory element

Michael Dambach[#1], **Melissa Sandoval**[#1,5], **Taylor B. Updegrove**[1], **Vivek Anantharaman**[3], **L. Aravind**[3], **Lauren S. Waters**[1,2,*], and **Gisela Storz**[1,*]

[1]Cell Biology and Metabolism Program, Eunice Kennedy Shriver National Institute of Child Health and Human Development, Bethesda, MD 20892-5430, USA

[2]Department of Chemistry, University of Wisconsin Oshkosh, Oshkosh, WI 54901, USA

[3]National Center for Biotechnology Information, National Library of Medicine, Bethesda, MD 20894, USA

[#] These authors contributed equally to this work.

SUMMARY

The highly-structured, *cis*-encoded RNA elements known as riboswitches modify gene expression upon binding a wide range of molecules. The *yybP-ykoY* motif was one of the most broadly distributed and numerous bacterial riboswitch whose cognate ligand was unknown. Using a combination of *in vivo* reporter and *in vitro* expression assays, equilibrium dialysis and northern analysis, we show that the *yybP-ykoY* motif responds directly to manganese ions in both *Escherichia coli* and *Bacillus subtilis*. The identification of the *yybP-ykoY* motif as a manganese ion sensor suggests the genes that are preceded by this motif, and encode a diverse set of poorly characterized membrane proteins, have roles in metal homeostasis.

Keywords

MntR; Fur; H-NS; translational regulation; cis-acting regulatory RNAs; metal transporters

[*]Correspondence: watersl@uwosh.edu (L.S.W.) and storzg@mail.nih.gov (G.S.).
[5]Present address: Biomedical Sciences Graduate Program, University of California, San Francisco, CA

AUTHOR CONTRIBUTIONS

M.D. and M.S. designed and performed the majority of the experiments and wrote the manuscript. T.B.U. helped with experiments to characterize in vitro synthesized RNA and helped write the manuscript, V.A. and L.A. carried out computational analysis of the *yybP-ykoY* motif and helped write the discussion, L.S.W. carried out experiments, guided the project and wrote the manuscript, and G.S. guided the project and wrote the manuscript.

INTRODUCTION

Transition metal ions are essential trace nutrients in all domains of life. The unique redox properties inherent to these metals make them ideal cofactors for a wide variety of enzymatic reactions (reviewed in (Finney and O'Halloran, 2003)). At excess levels, however, the reactive character of these ions simultaneously poses a potential threat to the cell (reviewed in (Finney and O'Halloran, 2003)). As a result, bacteria have evolved exquisite mechanisms to control transition metal homeostasis (reviewed in (Waldron and Robinson, 2009)). A key component of this homeostasis is the regulated import and export by high affinity transporters. Bacterial cells also possess highly sensitive regulatory strategies to modulate the synthesis of these transporters and other metal binding proteins (reviewed in (Waldron and Robinson, 2009)). For example, in many bacteria, the Fur and MntR transcription factors repress gene expression in response to high levels of iron and manganese, respectively (reviewed in (Waldron and Robinson, 2009)).

The cellular roles of iron and manganese are intertwined. Iron is a critical cofactor of many enzymes. However, when iron levels are low or cells are subject to oxidative stress leading to the detrimental, iron-catalyzed Fenton reaction, the synthesis of manganese-dependent isozymes is increased in *E. coli*. In addition, manganese is substituted in several iron-containing enzymes allowing continued activity (reviewed by Imlay, 2014). On the other hand, high levels of manganese can be detrimental for the same reason; in this case the manganese is substituted for iron in enzymes in which the substitution cannot be tolerated (Martin et al., 2015).

Given the benefits as well as the potential toxicity of manganese, transport of this transition metal is tightly controlled in *E. coli*. Expression of the major manganese importer encoded by *mntH* is repressed by both Fur and MntR and activated by the hydrogen peroxide-responsive transcription activator OxyR (Ikeda et al., 2005; Kehres et al., 2002; Patzer and Hantke, 2001). We recently discovered that *E. coli* cells also possess a manganese exporter encoded by the *mntP* gene and found that the levels of both the *mntP* mRNA and MntP protein increase in the presence of high manganese (Waters et al., 2011). Binding sites for both Fur and MntR were predicted upstream of the promoter for this gene (Chen et al., 2007; Ikeda et al., 2005; Kehres et al., 2002; Stojiljkovic et al., 1994), but it was not clear how these two repressors activate *mntP* expression. It was also noted that the 5′-untranslated region (5′-UTR) of the *mntP* gene is unusually long and contains a conserved riboswitch element of the *yybP-ykoY* family (Barrick et al., 2004).

Riboswitches are *cis*-acting regulatory RNAs most commonly embedded in the 5′-UTRs of the genes that they regulate (reviewed in (Serganov and Nudler, 2013)). These structured RNA elements are comprised of two components: a highly conserved ligand-binding aptamer domain and a variable expression platform that executes genetic regulation. Upon binding of their cognate ligand(s), most riboswitches modify gene expression through one of two mechanisms: transcription regulation by controlling formation of an intrinsic transcription terminator or translation initiation by controlling the sequestration of ribosome binding sites.

To date, there are more than 25 experimentally validated riboswitch classes, which sense and respond to diverse compounds including enzymatic cofactors, nucleotide derivatives, amino acids, sugars, as well as Mg^{2+} and F^{-} ions (reviewed in (Breaker, 2011; Serganov and Nudler, 2013)). In addition, the explosion of sequenced bacterial genomes coupled with the highly conserved primary sequence and secondary structure of riboswitch aptamer domains have facilitated the bioinformatic identification of nearly two dozen putative "orphan" riboswitch classes whose ligands have yet to be identified. Of these orphan riboswitches, the *yybP-ykoY* motif is by far the most numerous (Meyer et al., 2011). The motif was first identified as preceding the *yybP* and *ykoY* genes in *Bacillus subtilis* (Barrick et al., 2004), but over 1,000 unique examples of the *yybP-ykoY* motif have been found to be broadly distributed across many bacterial phyla (Meyer et al., 2011; Sun et al., 2013). Typically, identification of the ligand sensed by an orphan riboswitch has been inferred from its genetic context (Winkler et al., 2002). However, for the *yybP-ykoY* riboswitch motif, which precedes genes predicted to encode membrane associated proteins, in particular cation transporters, permeases and poorly understood TerC membrane proteins that contribute to tellurium resistance, did not offer coherent clues as to the compound being sensed by this regulatory RNA (Barrick et al., 2004; Meyer et al., 2011). There are two copies of the *yybP-ykoY* motif in *E. coli*; one upstream of *mntP* and one upstream of *alx*, which encodes a member of the TerC superfamily (Anantharaman et al., 2012). Since we found *mntP* to be manganese-inducible, we wondered whether the *yybP-ykoY* motif responded to manganese.

To elucidate the mechanism of *mntP* induction by manganese, we assayed *lacZ* fusions to the *mntP* promoter and 5′-UTR. Assays of transcriptional fusions showed that Fur and MntR activate the *mntP* promoter by counteracting the repressive effects of the histone-like H-NS protein. Assays of wild type and mutant translational fusions together with biochemical studies revealed that the 5′-UTR directly binds and responds to manganese. Based on the expression of an *alx* 5′-UTR-*lacZ* fusion in *E. coli* and the *ykoY* and *yybP* mRNAs in *Bacillus subtilis*, we propose that this orphan riboswitch family broadly responds to manganese and discuss the implications of our findings for the large families of membrane proteins whose genes are preceded by the *yybP-ykoY* motif.

RESULTS

The *mntP* promoter and 5′-UTR independently contribute to *mntP* induction by Mn^{2+}

To begin to dissect *mntP* induction by $MnCl_2$, we first generated $P_{mntP660}$-$5'UTR_{mntP}$-*lacZ* fusions containing the entire *mntP* promoter region beginning 660 nucleotides (nt) upstream of the transcription start site, the 225 nt *mntP* 5′-UTR containing the riboswitch homology, and the first 15 amino acids of the MntP open reading frame (ORF) fused to *lacZ* (Figure 1A). The strain with a $P_{mntP660}$-$5'UTR_{mntP}$-*lacZ* translational fusion (i) (for which translation is dependent on the *mntP* ribosome binding site) showed a profound increase in activity (61.7-fold) with 400 μM $MnCl_2$ in LB medium (Figure 1B). Cells bearing a $P_{mntP660}$-$5'UTR_{mntP}$-*lacZ* transcriptional fusion (ii) (for which translation is dependent on the *lacZ* ribosome binding site) also showed $MnCl_2$-dependent induction but to a lower extent (3.9-fold) and had significantly higher basal activity without $MnCl_2$. These data

demonstrate $MnCl_2$-dependent regulation of *mntP* at both the transcriptional and translational levels.

The individual contributions of the *mntP* promoter and 5′-UTR were assessed with three additional fusions: a $P_{mntP660}$-*lacZ* promoter fusion (iii) comprising the 660 nt upstream of the transcription start site fused to the *lacZ* transcript (which lacks the *mntP* 5′-UTR) and P_{LlacO}-5′UTR$_{mntP}$-*lacZ* transcriptional (iv) and translational (v) 5′-UTR fusions consisting of the 225 nt 5′-UTR and the first 15 amino acids of MntP under the control of a heterologous promoter, P_{LlacO} (Figure 1B). Exposure to $MnCl_2$ induced the $P_{mntP660}$-*lacZ* promoter fusion (iii) (2.5-fold). The P_{LlacO}-5′UTR$_{mntP}$-*lacZ* translational fusion (iv) also showed $MnCl_2$-dependent induction (7.9-fold), but the P_{LlacO}-5′UTR$_{mntP}$-*lacZ* transcriptional fusion (v) did not. Thus the promoter and 5′-UTR of *mntP* independently contribute to $MnCl_2$-dependent regulation, and the 5′-UTR affects translation initiation rather than transcription termination.

Both the *mntP* promoter and 5′-UTR respond specifically to Mn^{2+}

To test whether the *mntP* promoter and 5′-UTR respond to metals other than Mn^{2+}, we also examined expression of the fusions in cells exposed to either Mg^{2+} or several divalent transition metals in minimal medium (Figures 1C and 1D) or the metalloid tellurium in LB medium (data not shown). The $P_{mntP660}$-*lacZ* promoter fusion (iii) was strongly induced by both 40 and 400 μM $MnCl_2$ and partially induced by 400 μM $FeSO_4$ and $CoCl_2$, though it is unlikely cells encounter 400 μM Co^{2+} under physiological conditions. The P_{LlacO}-5′UTR$_{mntP}$-*lacZ* translational fusion (iv) showed a concentration dependent induction with $MnCl_2$, but not with any of the other transition metals or K_2TeO_3. These data indicate that *in vivo*, the *mntP* promoter is strongly regulated by Mn^{2+} and partially by Fe^{2+} while the *mntP* riboswitch specifically responds to Mn^{2+}.

MntR and Fur activate the *mntP* promoter by antagonizing H-NS

To define the regions of the *mntP* promoter required for the induction by $MnCl_2$, we generated a shorter promoter fusion, $P_{mntP264}$-*lacZ* (vi), comprising the 264 nt upstream of the transcription start site fused to *lacZ*. This fusion still possesses two MntR consensus binding sites centered at 147 and 187 nt upstream of the transcription start site (Ikeda et al., 2005; Kehres et al., 2002; Yamamoto et al., 2011) as well as a Fur binding site centered at 75 nt upstream of the transcription start site (Stojiljkovic et al., 1994) (Figure 2A). Surprisingly, the shorter promoter fusion showed higher basal expression and very low inducibility by $MnCl_2$ (1.3-fold) in minimal medium (Figure 2B). The region upstream of the MntR binding sites has been observed to bind to the H-NS nucleoid-binding protein in *E. coli* and *Salmonella enterica* (Navarre et al., 2006; Oshima et al., 2006). We thus hypothesized that H-NS might bind upstream of *mntP* and that MntR and Fur might antagonize this H-NS-mediated repression, analogous to what has been observed for H-NS repression and Fur-dependent activation of the *ftnA* gene (Nandal et al., 2010). We tested this hypothesis by assaying [.beta]-galactosidase activity from the $P_{mntP660}$-*lacZ* transcriptional fusion (iii) in wild-type, Δ*hns*, Δ*mntR*, Δ*fur* and Δ*mntR* Δ*fur* mutant cells. We found that the activity of the $P_{mntP660}$-*lacZ* transcriptional fusion was constitutively high in both the absence and presence of $MnCl_2$ in the Δ*hns* strain, suggesting that H-NS does

indeed negatively affect *mntP* expression (Figure 2C). In contrast, $MnCl_2$-dependent induction was significantly reduced in the Δ*mntR* and Δ*fur* backgrounds, and was completely abolished in the Δ*mntR* Δ*fur* double mutant. Thus the two repressors, Mn^{2+}-binding MntR and Fur, which has been shown to be loaded with Mn^{2+} when the metal is present at high concentrations (Martin et al., 2015), activate transcription by antagonizing the repressive effects of H-NS at the *mntP* promoter.

Mutations of conserved residues in the *mntP* aptamer abolish regulation by Mn^{2+} in vivo and in vitro

Next we sought to characterize the Mn^{2+}-responsive *mntP* 5′-UTR. We first concentrated on the highly conserved part of the *mntP* 5′-UTR (nt 1-110) that corresponds to the *yybP-ykoY* aptamer motif (Figure S1A). The remainder of the 5′-UTR (nt 111-225) is more variable and is predicted to serve as the expression platform. Figure 3A depicts the secondary structure of the first 110 nt of the *mntP* 5′-UTR generated using the *yybP-ykoY* consensus structure (Barrick et al., 2004) and supported by enzymatic and lead structure probing (Figure S2). To test the contributions of specific nucleotides in this aptamer domain to $MnCl_2$ responsiveness, we generated multiple P_{LlacO}-5′UTR_{mntP}-*lacZ* translational fusions (iv) carrying mutations of three sets of residues that were greater than 97% conserved in the *yybP-ykoY* consensus structure (G_9G_{10}, $C_{49}A_{50}$, and $A_{101}G_{102}A_{103}$) (Meyer et al., 2011). We also mutated another set of residues that were only conserved among closely related enteric bacteria ($A_{27}U_{28}U_{29}$). $MnCl_2$-dependent induction of fusion gene expression was almost completely abolished by mutations in the three sets of highly conserved residues, while wild type induction was observed for the fusion carrying mutations in the less conserved residues (Figure 3B).

We also tested the synthesis of a MntP-SPA fusion protein in an in vitro translation assay using in vitro synthesized RNA templates encompassing the wild type aptamer, the mutant aptamers described above, and a constitutively active mutant aptamer described below. Consistent with our in vivo assays, the addition of $MnCl_2$ induced synthesis of the MntP-SPA fusion protein with the wild type and $A_{27}U_{28}U_{29}$ mutant templates, while mutations in the highly conserved nucleotides G_9G_{10} and $C_{49}A_{50}$ and $A_{101}G_{102}A_{103}$ eliminated induction by $MnCl_2$ (Figure 3C). In contrast, when we used the mutant with substitutions of $A_{200}U_{201}$, which displayed constitutively high levels of *lacZ* activity even without $MnCl_2$ (see below), we observed high levels of MntP-SPA in both the absence and presence of $MnCl_2$. Importantly, these in vitro assays show that, in a minimal expression system, the addition of $MnCl_2$ alone was sufficient to promote translation of the *mntP* transcript. Together, the results of the in vivo and in vitro expression assays support the conclusion that the *mntP* riboswitch directly senses and responds to Mn^{2+}.

The *mntP* 5′-UTR binds Mn^{2+}

To test whether the *mntP* aptamer directly binds Mn^{2+}, we carried out equilibrium dialysis followed by atomic absorption spectroscopy (Table 1 and Table S1). In these assays, 100 μM in vitro transcribed wild type or $C_{49}A_{50}$ mutant aptamer (nt 1-110) RNA, 50 μM of the double stranded DNA template used to synthesize the wild type RNA or 100 μM of an unrelated cyclic dinucleotide (c-di-GMP) binding aptamer (Kulshina et al., 2009), all in

buffer containing 20 mM $MgCl_2$, were placed in dialysis chambers opposite a second chamber with only the buffer. After a range of $MnCl_2$ concentrations was introduced into the buffer-only side, the samples were equilibrated for 48 h. The solution in each of the dialysis chambers was then subjected to atomic absorption spectroscopy to quantitate Mn^{2+} levels. If the RNA or DNA specifically bound to Mn^{2+}, the metal would be enriched in the chamber containing the nucleic acids.

Strikingly, for the wild type aptamer, 93-100% of the Mn^{2+} added to the buffer side of the dialysis chamber was associated with the RNA after the incubation. In contrast, only 60-73% of the Mn^{2+} was associated with the $C_{49}A_{50}$ mutant. The partial binding by the $C_{49}A_{50}$ mutant might be explained by the existence of multiple Mn^{2+} binding sites, similar to the multiple Mg^{2+} binding "cores" reported for M-box riboswitches (Wakeman et al., 2009). The presence of only 59-60% of the Mn^{2+} in the chamber with DNA or c-di-GMP aptamer (approximately half, as expected in the absence of binding) suggests that nonspecific association of Mn^{2+} with nucleic acids is limited and does not explain the near 100% retention of Mn^{2+} by the wild type aptamer. These data confirm that the aptamer can directly bind Mn^{2+}.

Other members of the *yybP-ykoY* riboswitch family also respond to Mn^{2+}

Given our findings that the *mntP* aptamer was responsive to and directly bound Mn^{2+}, we examined the $MnCl_2$ responsiveness of other members of this broadly conserved family of orphan riboswitches. A paralog of the *yybP-ykoY* aptamer is found in the 5′-UTR of the *E. coli alx* gene (Barrick et al., 2004), which is predicted to code for an inner membrane protein of the TerC superfamily. The *alx* gene previously was found to be induced under alkaline conditions (Bingham et al., 1990). Fusions to *lacZ* and structure probing of wild type and mutant derivatives indicated that the *alx* 5′-UTR changes conformation in response to high pH, resulting in increased translation of the Alx protein (Nechooshtan et al., 2014; Nechooshtan et al., 2009). To assess the manganese responsiveness of the *alx* 5′-UTR, we constructed a P_{LlacO}-5′UTR$_{alx}$-*lacZ* translational fusion carrying the 5′-UTR and first 10 codons of *alx* fused to codon 10 of *lacZ*, similar to our P_{LlacO}-driven *mntP*-translational fusion. When exponentially growing cells harboring this construct were incubated with 4, 40, 400 or 4,000 μM $MnCl_2$, we observed an increase in [.beta]-galactosidase expression (Figure 4A) suggesting that, similar to the *mntP* 5′-UTR, the *yybP-ykoY* riboswitch preceding the *alx* ORF is responsive to Mn^{2+}.

Interestingly, while induction of the P_{LlacO}-5′UTR$_{mntP}$-*lacZ* translational fusion was proportional to the $MnCl_2$ concentration, the dose response curve for the P_{LlacO}-5′UTR$_{alx}$-*lacZ* translational fusion was different. The *alx* fusion showed only 2-3 fold induction by 4, 40 and 400 μM $MnCl_2$, but a robust 10-fold induction by 4,000 μM $MnCl_2$. Consistent with this in vivo result, the *alx* aptamer also showed less $MnCl_2$ binding than the *mntP* aptamer in equilibrium dialysis experiments (Table S1).

For the *yybP* and *ykoY* genes, the latter of which also codes for a member of the TerC superfamily in the Gram-positive *B. subtilis* (Barrick et al., 2004), effector binding to the aptamers was predicted to prevent formation of Rho-independent transcription terminators (Figure S3C-D). To test this prediction, we carried out northern analysis to examine the

yybP and *ykoY* transcripts present in total RNA isolated from stationary phase cells left untreated or supplemented with 40 and 400 μM $MnCl_2$ for 1 h. Using labeled oligonucleotides complementary to the *yybP* and *ykoY* aptamers, we observed prominent low molecular weight bands (~90 and ~140 nt for *yybP* and ~160 nt for *ykoY*) corresponding to the aptamer domains in untreated cells (Figure 4B). The intensities of these bands decreased upon the addition of $MnCl_2$ with the concurrent emergence of higher molecular weight species. In the presence of 400 μM $MnCl_2$, a distinct band of the predicted size was observed for the ~600 nt *yybP* gene (Figure 4B), and a smear of higher molecular weight bands was detected upon overexposure for the >1,000 nt *ykoY* gene (Figure S3A). A previous microarray analysis of *B. subtilis* cells exposed to 2.5 μM $MnCl_2$ for 30 min reported 4- and 6-fold increases in *yybP* and *ykoY* respectively, though the abundance of each of these full-length transcripts was very low (Guedon et al., 2003). All of these observations indicate that the *yybP* and *ykoY* aptamers also respond to Mn^{2+} resulting in transcriptional read-through of the terminators resident in the expression platforms of these 5′-UTRs.

Change in ribosome accessibility leads to the activation of *mntP* translation

After characterizing the aptamer region, we next turned to the expression platform and the mechanism of the Mn^{2+}-dependent activation of *mntP* translation. Given that secondary structural changes to the *alx*, *yybP* and *ykoY* riboswitches upon ligand binding are predicted to affect a stem-loop at the 3′ end of the aptamer domain (Figure S3B-D) and the observed conservation of base pairing in the *mntP* leader (Figure S1A), we predicted a secondary structure in which the annotated *mntP* start codon is sequestered by base pairing in the absence but not the presence of Mn^{2+} (Figure 5A). Toeprinting experiments (Figure 5B) confirmed that 30S ribosomes bind at the annotated AUG only in the presence of 400 μM $MnCl_2$, further supporting the conclusion that *mntP* translation is directly affected by Mn^{2+} binding. Additionally, mutation of two possible upstream alternate start codons, which are preceded by GA-rich sequences and show ribosome binding in ribosome profiling experiments (Li et al., 2012), did not affect expression of P_{LlacO}-5′UTR$_{mntP}$-*lacZ* translation fusion (Figure S1B), suggesting Mn^{2+} binding does not affect a stand-by ribosome or translation of a leader peptide.

To test our model, we mutated residues in the long conserved stem overlapping the 3′end of the aptamer ($A_{106}U_{107}$ to $U_{106}A_{107}$ and $A_{200}U_{201}$ to $U_{200}A_{201}$) in the context of the P_{LlacO}-5′UTR$_{mntP}$-*lacZ* translational fusion. This stem is also present in the *alx*, *yybP*, and *ykoY* riboswitches and is predicted to be altered in the “off” versus “on” state (Figure S3B-D). Consistent with a role for this stem in repressing *mntP* translation, expression was constitutively high in the single mutants and restored to lower levels in the double mutant (Figure 5C). Possible interference of the $U_{106}A_{107}$ mutations in Mn^{2+} binding might explain the loss of Mn^{2+} induction in the double mutant. We also mutated, separately and in combination, conserved G-rich ($U_{180}G_{181}G_{182}G_{183}$ to $A_{180}C_{181}C_{182}C_{183}$) and C-rich ($C_{208}C_{209}C_{210}G_{211}$ to $G_{208}G_{209}G_{210}U_{211}$) sequences predicted to be basepaired in the “on” state (Figure 5D). For the single mutants, induction by $MnCl_2$ was significantly reduced compared to the wild type fusion. Induction was increased in the double mutant, which had constitutively high basal expression. These mutational data are consistent with a Mn^{2+}-

induced structural change that prevents formation of a stem-loop structure, which sequesters the ribosome-binding site of *mntP*, allowing for translation.

We also examined the structures of the 5′-UTRs of the wild type and the $C_{49}A_{50}$ reduced-binding mutant by lead-mediated cleavage, which preferentially affects flexible RNA regions. These structure-probing reactions were carried out in the presence and absence of $MnCl_2$. Limited Mn^{2+}-dependent changes were observed in the wild type aptamer domain (Figure 5E and Figure S4); the A_{34}, A_{35}, C_{46}, A_{47}, G_{77} and G_{102} residues showed somewhat less cleavage in the presence of Mn^{2+}. These differences were not detected for the $C_{49}A_{50}$ mutant. More extensive changes were observed for the expression platform where nucleotides between A_{106} and G_{110} as well as U_{196} and G_{202} showed increased $MnCl_2$-dependent lead cleavage for the wild type 5′-UTR but not the $C_{49}A_{50}$ mutant (Figure 5E). The increased cleavage observed in these regions in the presence of Mn^{2+} is consistent with the predicted increase in flexibility of these sequences in the “on” secondary structure, which again would facilitate ribosome binding and translation.

DISCUSSION

We have shown that the *mntP* promoter and 5′-UTR independently respond to Mn^{2+}, leading to increased expression of the MntP manganese exporter at both the transcriptional and translational levels. At the promoter, MntR and Fur antagonize the repressive effects of H-NS binding when cells are exposed to high Mn^{2+}. Within the 5′-UTR, the *yybP-ykoY* riboswitch directly binds Mn^{2+}, resulting in a conformation that liberates the ribosome-binding site. This finding of dual regulation raises questions about the advantages of positively regulating both transcription and translation in response to the same ligand. We suggest that the tight control highlights how precise regulation of intracellular Mn^{2+} levels is critical to cells.

Additionally, we have also shown that other homologs of the *yybP-ykoY* riboswitch also confer Mn^{2+}-dependent gene regulation through a transcription termination mechanism. These experiments along with a parallel structural study (Price et al., 2014), are the first demonstration of a ligand for this orphan riboswitch class. The Mn^{2+}-sensing capability of the *yybP-ykoY* motif, together with the newly-discovered NiCo motif which is responsive to Co^{2+} and Ni^{2+} (Furukawa et al., 2015) and another possible Mn^{2+} binding riboswitch repressing the *S. enterica mntH* gene (Shi et al., 2014), reveal that riboswitches can directly sense and respond to transition metals. We suggest that other less broadly-conserved RNA motifs may be found to recognize still other transition metals.

yybP-ykoY riboswitches exhibit unique properties

A number of features distinguish the *yybP-ykoY* family from the majority of riboswitch classes studied to date. First, in contrast to most characterized riboswitches, only minimal structural changes to the aptamer are observed upon Mn^{2+} binding as assessed by both lead and inline probing. For the latter, only one change, increased cleavage at G_{33}, was detected in the aptamer domain (Figure S4C and D). It is possible that the Mg^{2+} present in the buffers masks some of the effects of Mn^{2+} binding given that these two ions can occupy the same binding sites in RNA tertiary structures (Ramesh et al., 2011), but increased cleavage at G_{33}

and A_{34} were the only inline probing changes observed in a buffer lacking Mg^{2+} (Figure S4E). Alternatively, the *yybP-ykoY* aptamer may adopt a preformed tertiary structure in the absence of Mn^{2+}. This would be reminiscent of lysine-responsive L-box riboswitches which display minor changes in spontaneous cleavage in response to lysine and have the same three dimensional crystal structure in the absence and presence of lysine (Garst et al., 2008; Serganov et al., 2008; Sudarsan et al., 2003). Interestingly, the NiCo riboswitch also is largely preformed in the absence of its ligand (Furukawa et al., 2015).

Another unusual feature of the *yybP-ykoY* motif is the overlap of the expression platform with the aptamer domain. Riboswitches usually have a "modular" structure with distinct aptamer and expression platform domains (Breaker, 2011). However, examination of the sequences of multiple *yybP-ykoY* family members reveals that in every instance in which this motif is predicted to affect transcription termination, a portion of the terminator stem corresponding to the expression platform is part of the highly conserved P4 helix of the aptamer (Barrick et al., 2004). This unique arrangement is also observed for many of the Class I c-di-GMP riboswitch family members that utilize Rho-independent transcription terminators (Weinberg et al., 2007). Unlike the majority of riboswitches which are genetic "off" switches, the *yybP-ykoY* riboswitches and the Class I c-di-GMP switches are all postulated to be genetic "on" switches (Barrick et al., 2004; Weinberg et al., 2007), as we have observed for *mntP* and *alx*.

We also note that the predicted first and third stem-loop structures of the *yybP-ykoY* motif can be quite varied. Although we found activation of *E. coli mntP* to be specific to Mn^{2+}, it is possible that members of this family respond to different concentrations of Mn^{2+} as appears to be the case for *mntP* and *alx*, different oxidation states of manganese, or even other cations. Members of this riboswitch family also may respond to environmental signals in addition to Mn^{2+} similar to the multi-layered regulation reported for the *mgtA* Mg^{2+}-responsive riboswitch (Park et al., 2010). Alkaline conditions have been reported to elevate the levels of the *alx, yybP* and *ykoY* transcripts and *alx* translation (Bingham et al., 1990; Nechooshtan et al., 2014; Nechooshtan et al., 2009; Wiegert et al., 2001). We also observed alkaline pH induction of P_{alx}-5′UTR_{alx}-*lacZ* transcriptional and translational fusions but not the P_{LlacO}-5′UTR_{alx}-*lacZ* translational fusion (data not shown). How Mn^{2+} and high pH signals overlap and affect expression of these genes will be an interesting topic for future research. In the case of *alx*, we suggest that Mn^{2+} binding prevents transcription termination, which leads to the accumulation of the short transcript identified as the SraL small RNA (Argaman et al., 2001), independent of the effects of high pH on transcription and translation.

Genes preceded by *yybP-ykoY* riboswitches are likely to have roles in metal homeostasis

Given the prevalence of the *yybP-ykoY* family of riboswitches, we sought to better understand their functional associations using the wealth of complete genome sequences from 2755 organisms (Table S2). We identified 1338 genomes with at least one significantly scoring *yybP-ykoY* motif and found a mean of 1.5 motifs per genome, revealing that a notable fraction of the genomes coded for two or more *yybP-ykoY* riboswitches. The motif is observed in most major bacterial clades but none of the archaeal clades, suggesting that it

first emerged in the bacterial common ancestor. Among the organisms having this riboswitch, we found enrichment for soil and aquatic bacteria. Moreover, even in clades where the motif is present, it is virtually absent in endo-parasitic and symbiotic bacteria. This distribution is consistent with a role for this riboswitch in responding to potentially toxic environmental metals.

Systematic classification of the genes associated with *yybP-ykoY* riboswitches confirmed that the motif is unique among riboswitch-regulated genes in having an almost exclusive association with genes encoding transmembrane or membrane-associated proteins, particularly transporters (Figures 6 and S5). Tallies of the downstream genes revealed that *terC* is the gene most frequently preceded by *yybP-ykoY* riboswitches. Earlier sequence analysis showed that TerC proteins have multiple conserved transmembrane segments, some of which are marked by a distinctive pattern of embedded acidic residues (Anantharaman et al., 2012). Thus the proteins could interact with cations within the membrane and function as metal transporters. The second hub is a P-type ATPase belonging to a distinct clade related to Ca^{2+}-efflux pumps (Chan et al., 2010). Interestingly, the genes encoding TerC and P-type ATPases almost never co-occur in the same genome downstream of paralogous *yybP-ykoY* motifs. This pattern of near complete mutual exclusivity between riboswitch-regulated TerC and the P-type ATPase genes suggests that they likely perform an equivalent function in divalent metal efflux in the genomes that code for them. Genomes with the P-type ATPase gene preceded by the riboswitch only infrequently showed the presence of a second paralogous *yybP-ykoY* motif, suggesting the ATPase might have a broader functional spectrum than TerC proteins. In contrast, riboswitch-proximal genes of the MntP family, the UPF0016 family and several other less prevalent families coding for different known or predicted metal-transporters often co-occur with riboswitch-regulated TerC encoding genes. Given that the MntP and UPF0016 families show mutual exclusivity with respect to each other in the genomes in which they are found, UPF0016 proteins are likely a new class of manganese transporters; a proposal that is further supported by comparable patterns of charged residues associated with the transmembrane segments in both of these families.

The overwhelming association of genes encoded downstream of *yybP-ykoY* riboswitches with membrane proteins known or predicted to participate in metal transport supports our conclusion that this genetic element is linked to regulation of transition metal efflux. However, the frequent presence of multiple, distinct metal transporters linked to paralogous copies of the riboswitch in the same genome suggests that there might be some functional diversification within the *yybP-ykoY* family.

In a limited number of instances, the *yybP-ykoY* motif is associated with a downstream gene encoding either a MetJ/Arc (ribbon-helix-helix) or a Zn-ribbon transcription factor (Aravind and Koonin, 1999). Some of these operons additionally code for membrane proteins immediately downstream of the predicted transcription factor. This arrangement suggests that these mRNAs may also be subject to two-levels of regulation by both the riboswitch and transcription factor as we observed for MntP.

An accompanying article presenting the crystal structure of the *yybP-ykoY* riboswitch indicates that specificity for Mn^{2+} is dependent in large part on the adenine corresponding to

A_{50} in the *mntP* 5′-UTR (Price et al., 2014). This residue is almost completely conserved suggesting manganese specificity is likely to be preserved across all representatives of the family. However, the riboswitch also has a second metal-binding site with lower specificity, which might be more prone to accepting other metals and could influence binding at the specific site. Manganese has a range of oxidation states, which vary with pH and voltage potential, and higher pH favors the prevalence of states such as Mn(III). Given the connection between the *yybP-ykoY* family and alkaline pH, the possibility that *yybP-ykoY*-associated gene products act on different states of the metal is intriguing.

Overall, our study points to a large set of poorly understood genes preceded by *yybP-ykoY* motifs whose further characterization in the context of manganese homeostasis undoubtedly will give insights into the cellular mechanisms used to protect against transition metal toxicity.

EXPERIMENTAL PROCEDURES

Strains

All strains and oligonucleotides used in this study are listed in Table S3. Strain construction and growth conditions are described in Supplemental Experimental Procedures.

β-galactosidase assays

For all β-galactosidase assays, three separate colonies grown overnight in LB or minimal M9 medium supplemented with 0.2% glucose, were diluted to OD_{600} ~0.01-0.025 in the indicated media and grown to OD_{600} ~0.2. If required, IPTG was added at a final concentration of 1 mM. Immediately following IPTG addition, cells were either left untreated or incubated with the indicated final metal concentrations. After a 60 min incubation, cells were harvested and assayed for β-galactosidase activity (Miller, 1992).

In vitro translation assays

The RNA templates were first synthesized using the MEGAscript T7 Transcription Kit (Ambion) according to manufacturer's instructions. The transcripts were treated with 8 Units of DNase for 30 min, purified over a G50 spin column, extracted with phenol-chloroform and ethanol precipitated before 1 μg of RNA was mixed with the PURExpress in vitro Protein Synthesis kit containing *E. coli* ribosomes (New England Biolabs).

Equilibrium dialysis and atomic absorption spectroscopy

Indicated in vitro synthesized RNA or DNA (PCR template used for RNA synthesis) in 75 μl of buffer consisting of 50 mM Tris pH 8.3, 100 mM KCl, and 20 mM $MgCl_2$ was placed into one chamber of a 5 kDa cutoff equilibrium dialysis chamber (Harvard Apparatus). The opposing chamber was loaded with buffer only and subsequently injected with 20 μM$MnCl_2$. The dialysis apparatus was incubated with rocking at room temperature for 48 h, whereupon the samples from both sides of the chamber were collected into separate tubes. All samples were diluted with nitric acid (final 6%) and incubated at 95°C for 16 h to extract Mn^{2+}. The concentration of $Mn^{2+}$was measured by the 4100ZL graphite furnace atomic absorption spectrometer equipped with AS-70 automatic sampler (Perkin Elmer). The

system was calibrated with standards of Mn^{2+} (AAMN1-1; 1000 +/− 10 μg/ml) obtained from Inorganic Ventures Inc. Measurements for each sample were carried out in triplicate and given as the mean ± standard deviation of the mean (SDM) of the three values.

RNA isolation and northern analysis

RNA was isolated and analyzed by northern analysis as in (Zhang et al., 2013); details are provided in Supplemental Experimental Procedures.

Toeprinting assay

Toeprinting assays were carried out as in (Altuvia et al., 1998); details are provided in Supplemental Experimental Procedures.

RNA radiolabeling and in vitro structure probing

Template DNA for T7 transcription was amplified from the MG1655 genome starting at the +1 of the 5′-UTR of *mntP* (225 nt upstream MntP ORF) to the 15th amino acid of the MntP ORF by PCR with primers containing the T7 promoter (TAATACGACTCACTATAGG). T7 transcription was conducted using the MegaShortscript T7 Transcription Kit (Ambion) according to manufacturer's instructions. In vitro structural probing with RNase T1 and lead (II) was preformed in 10 μl reactions as in (Beisel et al., 2012).

Supplementary Material

Refer to Web version on PubMed Central for supplementary material.

ACKNOWLEDGMENTS

We thank S. Altuvia, N. Baird, A. Banerjee, A. Ferre-d'Amare, S. Gottesman, J. Imlay, B. Rosen, W. Winkler and J. Zhang for helpful discussions, and D.-Y. Lee for the atomic absorbance analysis. This work was supported by the Intramural Research Programs of the Eunice Kennedy Shriver National Institute of Child Health and Human Development and the National Library of Medicine as well as the Pharmacology Research Associate Program (L.S.W.) and the National Institutes of Health Undergraduate Scholarship Program (M.S.).

REFERENCES

Altuvia S, Zhang A, Argaman L, Tiwari A, Storz G. The Escherichia coli OxyS regulatory RNA represses fhlA translation by blocking ribosome binding. EMBO J. 1998; 17:6069–6075. [PubMed: 9774350]

Anantharaman V, Iyer LM, Aravind L. Ter-dependent stress response systems: novel pathways related to metal sensing, production of a nucleoside-like metabolite, and DNA-processing. Mol Biosyst. 2012; 8:3142–3165. [PubMed: 23044854]

Aravind L, Koonin EV. DNA-binding proteins and evolution of transcription regulation in the archaea. Nucleic Acids Res. 1999; 27:4658–4670. [PubMed: 10556324]

Argaman L, Hershberg R, Vogel J, Bejerano G, Wagner EGH, Margalit H, Altuvia S. Novel small RNA-encoding genes in the intergenic regions of Escherichia coli. Curr Biol. 2001; 11:941–950. [PubMed: 11448770]

Barrick JE, Corbino KA, Winkler WC, Nahvi A, Mandal M, Collins J, Lee M, Roth A, Sudarsan N, Jona I, et al. New RNA motifs suggest an expanded scope for riboswitches in bacterial genetic control. Proc Natl Acad Sci USA. 2004; 101:6421–6426. [PubMed: 15096624]

Beisel CL, Updegrove TB, Janson BJ, Storz G. Multiple factors dictate target selection by Hfq-binding small RNAs. EMBO J. 2012; 31:1961–1974. [PubMed: 22388518]

Bingham RJ, Hall KS, Slonczewski JL. Alkaline induction of a novel gene locus, alx, in Escherichia coli. J Bacteriol. 1990; 172:2184–2186. [PubMed: 2108134]

Breaker RR. Prospects for riboswitch discovery and analysis. Mol Cell. 2011; 43:867–879. [PubMed: 21925376]

Chan H, Babayan V, Blyumin E, Gandhi C, Hak K, Harake D, Kumar K, Lee P, Li TT, Liu HY, et al. The p-type ATPase superfamily. J Mol Microbiol Biotechnol. 2010; 19:5–104. [PubMed: 20962537]

Chen Z, Lewis KA, Shultzaberger RK, Lyakhov IG, Zheng M, Doan B, Storz G, Schneider TD. Discovery of Fur binding site clusters in Escherichia coli by information theory models. Nucleic Acids Res. 2007; 35:6762–6777. [PubMed: 17921503]

Finney LA, O'Halloran TV. Transition metal speciation in the cell: insights from the chemistry of metal ion receptors. Science. 2003; 300:931–936. [PubMed: 12738850]

Furukawa K, Ramesh A, Zhou Z, Weinberg Z, Vallery T, Winkler WC, Breaker RR. Bacterial riboswitches cooperatively bind Ni^{2+} or Co^{2+} ions and control expression of heavy metal transporters.. 2015 submitted.

Garst AD, Héroux A, Rambo RP, Batey RT. Crystal structure of the lysine riboswitch regulatory mRNA element. J Biol Chem. 2008; 283:22347–22351. [PubMed: 18593706]

Guedon E, Moore CM, Que Q, Wang T, Ye RW, Helmann JD. The global transcriptional response of *Bacillus subtilis* to manganese involves the MntR, Fur, TnrA and s^B regulons. Mol Microbiol. 2003; 49:1477–1491. [PubMed: 12950915]

Ikeda JS, Janakiraman A, Kehres DG, Maguire ME, Slauch JM. Transcriptional regulation of sitABCD of Salmonella enterica serovar Typhimurium by MntR and Fur. J Bacteriol. 2005; 187:912–922. [PubMed: 15659669]

Kehres DG, Janakiraman A, Slauch JM, Maguire ME. Regulation of Salmonella enterica serovar Typhimurium mntH transcription by H_2O_2, Fe^{2+}, and Mn^{2+}. J Bacteriol. 2002; 184:3151–3158. [PubMed: 12029030]

Kulshina N, Baird NJ, Ferré-D'Amaré AR. Recognition of the bacterial second messenger cyclic diguanylate by its cognate riboswitch. Nat Struct Mol Biol. 2009; 16:1212–1217. [PubMed: 19898478]

Li GW, Oh E, Weissman JS. The anti-Shine-Dalgarno sequence drives translational pausing and codon choice in bacteria. Nature. 2012; 484:538–541. [PubMed: 22456704]

Martin JE, Waters LS, Storz G, Imlay JA. The *Escherichia coli* protein MntS and exporter MntP collaborate to keep intracellular manganese at sufficient but sub-inhibitory levels. PLoS Genet. Mar 9.2015

Meyer MM, Hammond MC, Salinas Y, Roth A, Sudarsan N, Breaker RR. Challenges of ligand identification for riboswitch candidates. RNA Biol. 2011; 8:5–10. [PubMed: 21317561]

Miller, JH. A Short Course in Bacterial Genetics: A Laboratory Manual and Handbook for Escherichia coli and Related Bacteria. Cold Spring Harbor Laboratory Press; Plainview, NY: 1992.

Nandal A, Huggins CC, Woodhall MR, McHugh J, Rodríguez-Quiñones F, Quail MA, Guest JR, Andrews SC. Induction of the ferritin gene (ftnA) of Escherichia coli by Fe^{2+}-Fur is mediated by reversal of H-NS silencing and is RyhB independent. Mol Microbiol. 2010; 75:637–657. [PubMed: 20015147]

Navarre WW, Porwollik S, Wang Y, McClelland M, Rosen H, Libby SJ, Fang FC. Selective silencing of foreign DNA with low GC content by the H-NS protein in Salmonella. Science. 2006; 313:236–238. [PubMed: 16763111]

Nechooshtan G, Elgrably-Weiss M, Altuvia S. Changes in transcriptional pausing modify the folding dynamics of the pH-responsive RNA element. Nucleic Acids Res. 2014; 42:622–630. [PubMed: 24078087]

Nechooshtan G, Elgrably-Weiss M, Sheaffer A, Westhof E, Altuvia S. A pH-responsive riboregulator. Genes Dev. 2009; 23:2650–2662. [PubMed: 19933154]

Oshima T, Ishikawa S, Kurokawa K, Aiba H, Ogasawara N. Escherichia coli histone-like protein H-NS preferentially binds to horizontally acquired DNA in association with RNA polymerase. DNA Res. 2006; 13:141–153. [PubMed: 17046956]

Park SY, Cromie MJ, Lee EJ, Groisman EA. A bacterial mRNA leader that employs different mechanisms to sense disparate intracellular signals. Cell. 2010; 142:737–748. [PubMed: 20813261]

Patzer SI, Hantke K. Dual repression by Fe^{2+}-Fur and Mn^{2+}-MntR of the mntH gene, encoding an NRAMP-like Mn^{2+} transporter in Escherichia coli. J Bacteriol. 2001; 183:4806–4813. [PubMed: 11466284]

Price IR, Gaballa A, Ding F, Helmann JD, Ke A. Mn^{2+}-sensing mechanisms of *yybP-ykoY* orphan riboswitches. Mol Cell submitted. 2015

Ramesh A, Wakeman CA, Winkler WC. Insights into metalloregulation by M-box riboswitch RNAs via structural analysis of manganese-bound complexes. J Mol Biol. 2011; 407:556–570. [PubMed: 21315082]

Serganov A, Huang L, Patel DJ. Structural insights into amino acid binding and gene control by a lysine riboswitch. Nature. 2008; 455:1263–1267. [PubMed: 18784651]

Serganov A, Nudler E. A decade of riboswitches. Cell. 2013; 152:17–24. [PubMed: 23332744]

Shi Y, Zhao G, Kong W. Genetic analysis of riboswitch-mediated transcriptional regulation responding to Mn^{2+} in Salmonella. J Biol Chem. 2014; 289:11353–11366. [PubMed: 24596096]

Stojiljkovic I, Bäumler AJ, Hantke K. Fur regulon in gram-negative bacteria. Identification and characterization of new iron-regulated Escherichia coli genes by a fur titration assay. J Mol Biol. 1994; 236:531–545. [PubMed: 8107138]

Sudarsan N, Wickiser JK, Nakamura S, Ebert MS, Breaker RR. An mRNA structure in bacteria that controls gene expression by binding lysine. Genes Dev. 2003; 17:2688–2697. [PubMed: 14597663]

Sun EI, Leyn SA, Kazanov MD, Saier MHJ, Novichkov PS, Rodionov DA. Comparative genomics of metabolic capacities of regulons controlled by cis-regulatory RNA motifs in bacteria. BMC Genomics. 2013; 14

Wakeman CA, Ramesh A, Winkler WC. Multiple metal-binding cores are required for metalloregulation by M-box riboswitch RNAs. J Mol Biol. 2009; 392:723–735. [PubMed: 19619558]

Waldron KJ, Robinson NJ. How do bacterial cells ensure that metalloproteins get the correct metal? Nature Rev. Microbiol. 2009:25–35. [PubMed: 19079350]

Waters LS, Sandoval M, Storz G. The Escherichia coli MntR miniregulon includes genes encoding a small protein and an efflux pump required for manganese homeostasis. J Bacteriol. 2011; 193:5887–5897. [PubMed: 21908668]

Weinberg Z, Barrick JE, Yao Z, Roth A, Kim JN, Gore J, Wang JX, Lee ER, Block KF, Sudarsan N, et al. Identification of 22 candidate structured RNAs in bacteria using the CMfinder comparative genomics pipeline. Nucleic Acids Res. 2007; 35:4809–4819. [PubMed: 17621584]

Wiegert T, Homuth G, Versteeg S, Schumann W. Alkaline shock induces the *Bacillus subtilis* σ^W regulon. Mol Microbiol. 2001; 41:59–71. [PubMed: 11454200]

Winkler WC, Nahvi A, Breaker RR. Thiamine derivatives bind messenger RNAs directly to regulate bacterial gene expression. Nature. 2002; 419:952–956. [PubMed: 12410317]

Yamamoto K, Ishihama A, Busby SJ, Grainger DC. The Escherichia coli K-12 MntR miniregulon includes dps, which encodes the major stationary-phase DNA-binding protein. J Bacteriol. 2011; 193:1477–1480. [PubMed: 21239586]

Zhang A, Schu DJ, Tjaden BC, Storz G, Gottesman S. Mutations in interaction surfaces differentially impact E. coli Hfq association with small RNAs and their mRNA targets. J Mol Biol. 2013; 425:3678–3697. [PubMed: 23318956]

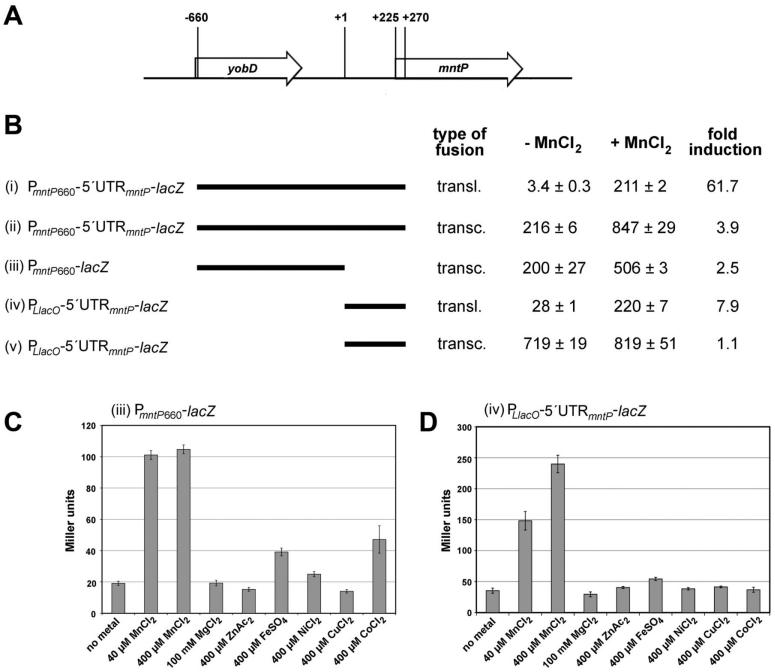

Figure 1. Transcription and translation of *mntP* are induced by $MnCl_2$

(A) Diagram of the *yobD-mntP* region. The numbering is as follows: +1 is the transcription start site, +225 corresponds to the AUG start codon, +270 shows the position of the fusion to the 15th amino acid.

(B) β-galactosidase activity for strains carrying chromosomal fusions with indicated *yobD-mntP* regions grown in LB medium and incubated without and with 400 µM $MnCl_2$ for 1 h. Transcriptional fusions (ii), (iii) and (v) rely on the *lacZ* ribosome-binding site and translational fusions (i) and (iv) rely on the *mntP* ribosome-binding site.

(C-D) β-galactosidase activity for strains carrying the $P_{mntP660}$-*lacZ* transcriptional (C) and the P_{LlacO}-5′UTR$_{mntP}$-*lacZ* translational (D) fusions grown in M9 glucose medium and incubated without or with indicated metals for 1 h.

For all β-galactosidase assays (B-D), the results are given in Miller units as the mean ± SDM of three independent samples.

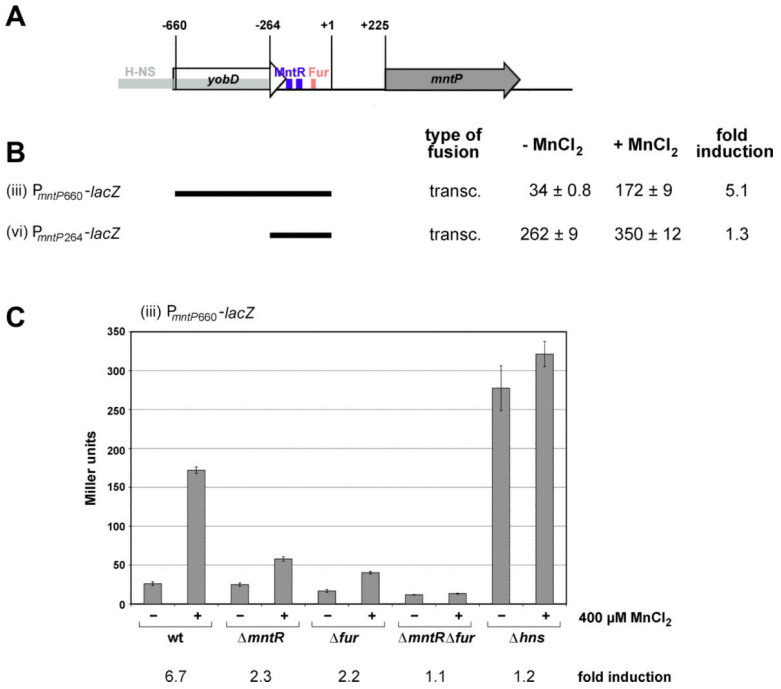

Figure 2. MntR and Fur antagonize H-NS binding

(A) Diagram of *yobD-mntP* chromosomal region with positions of H-NS, MntR and Fur binding sites indicated. Numbering is as in Figure 1.

(B) β-galactosidase activity for strains carrying transcriptional fusions with indicated *yobD-mntP* regions grown in M9 glucose medium and incubated without and with 400 µM $MnCl_2$ for 1 h.

(C) β-galactosidase activity for strains grown as in (B) carrying the $P_{mntP660}$-*mntP-lacZ* transcriptional fusion and indicated Δ*mntR*, Δ*fur* and Δ*hns* deletions.

For all β-galactosidase assays (B-C), the results are given in Miller units as the mean ± SDM of three independent samples.

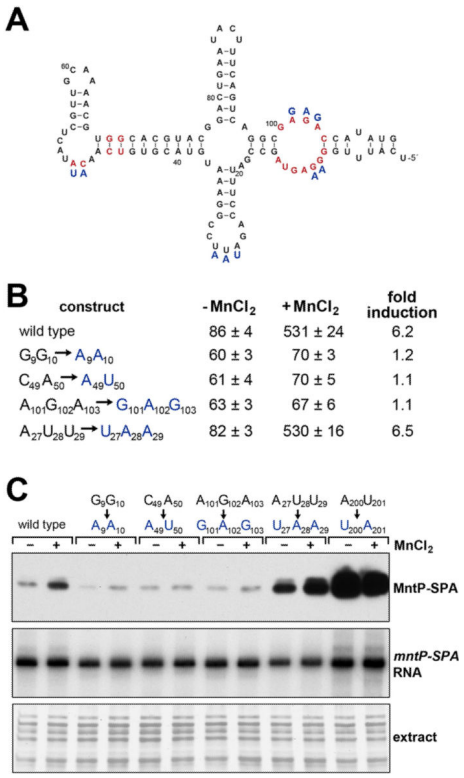

Figure 3. *mntP* riboswitch responds to $MnCl_2$ in vivo and in vitro

(A) Predicted secondary structure of the *mntP* aptamer based on conservation and structure probing. Nucleotides in red are conserved in >97% of the *yybP-ykoY* family members (Meyer et al., 2011). Blue letters correspond to mutants assayed in (B-C). See also Figure S1A and Figure S2.

(B) β-galactosidase activity for strains carrying P_{LlacO}-5′UTR_{mntP}-*lacZ* translational fusions with mutations of indicated residues grown in M9 glucose medium and incubated without and with 400 μM $MnCl_2$ for 1 h. The results are given in Miller units as the mean ± SDM of three independent samples.

(C) Reconstitution of *mntP* responsiveness to manganese in vitro with a purified *E. coli* in vitro translation system. Wild type or mutant RNA (1 μg) encompassing the *mntP* 5′-UTR and *mntP* ORF with a C-terminal SPA tag was incubated in the presence of no metal or 400 μM $MnCl_2$ for 2 h and then subjected to western blot analysis. The levels of the *mntP-SPA* mRNA were determined by primer extension analysis. The proteins were detected by silver staining of the gel after the transfer of the lower molecular weight proteins.

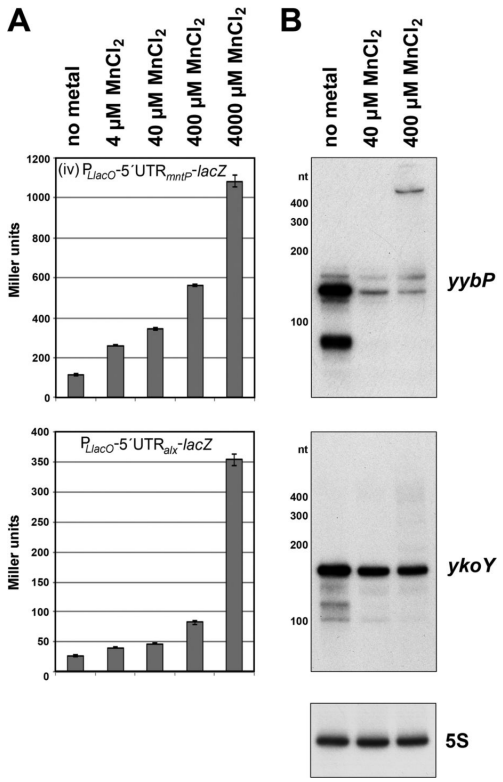

Figure 4. *E. coli* and *B. subtilis yybP-ykoY* paralogs respond to $MnCl_2$ in vivo

(A) β-galactosidase activity for *E. coli* strains carrying either a P_{LlacO}-5′UTR$_{mntP}$-*lacZ* or a P_{LlacO}-5′UTR$_{alx}$-*lacZ* translational fusion. Cells were grown in LB medium without or with 4, 40, 400 or 4,000 µM $MnCl_2$. The results are given in Miller units as the mean ± SDM of three independent samples.

(B) Northern blot analysis of the *B. subtilis yybP* and *ykoY* transcripts.

Total RNA was isolated from wild type *B. subtilis* stationary phase cells incubated with 40 or 400 µM$MnCl_2$ for 1 h. A blot with the RNA was probed with oligonucleotides specific to either the *yybP* or *ykoY* aptamer domain or 5S RNA. In the absence of added $MnCl_2$, bands corresponding to the sizes of the expected termination products of ~140 nt and ~160 nt for *yybP* and *ykoY*, respectively, are observed. Upon the addition of $MnCl_2$, higher molecular weight read-through products are detected with concomitant decreases in the lower molecular weight band. See also Figure S3A.

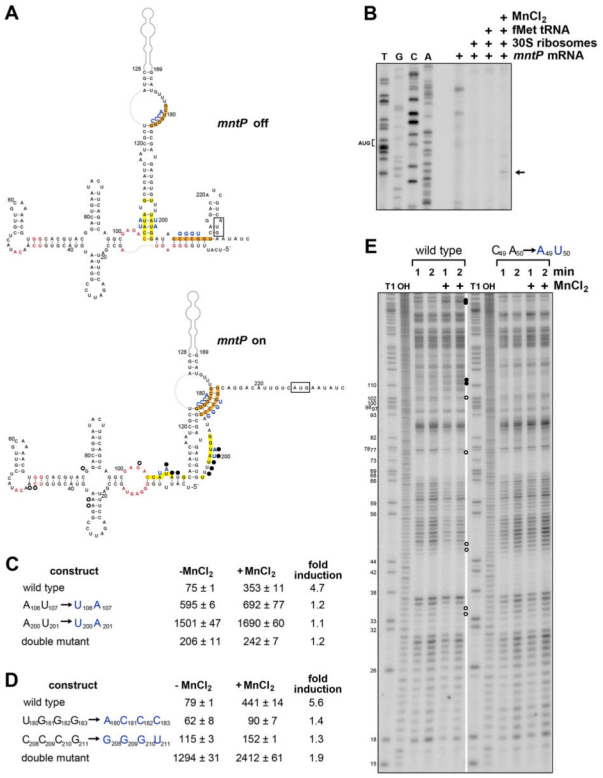

C

construct	-$MnCl_2$	+$MnCl_2$	fold induction
wild type	75 ± 1	353 ± 11	4.7
$A_{106}U_{107} \rightarrow U_{106}A_{107}$	595 ± 6	692 ± 77	1.2
$A_{200}U_{201} \rightarrow U_{200}A_{201}$	1501 ± 47	1690 ± 60	1.1
double mutant	206 ± 11	242 ± 7	1.2

D

construct	- $MnCl_2$	+ $MnCl_2$	fold induction
wild type	79 ± 1	441 ± 14	5.6
$U_{182}G_{183} \rightarrow A_{182}C_{183}$	62 ± 8	90 ± 7	1.4
$C_{209}C_{210}C_{211} \rightarrow G_{209}G_{210}G_{211}$	115 ± 3	152 ± 1	1.3
double mutant	1294 ± 31	2412 ± 61	1.9

Figure 5. Accessibility of *mntP* ribosome binding site changes upon manganese binding

(A) Predicted secondary structure of the complete *mntP* 5′-UTR from *E. coli*. The start codon is boxed, nucleotides conserved in >97% of the *yybP-ykoY* family members are in red (Meyer et al., 2011), regions predicted to base pair in the absence of Mn^{2+} are highlighted in yellow, while regions predicted to base pair in the presence of Mn^{2+} are highlighted in orange, and blue letters correspond to mutants assayed in (C-D). Nucleotides whose levels increase in a Mn^{2+}-dependent manner in (E) are indicated with filled circles, nucleotides whose levels decrease are indicated with open circles. See also Figure S4.

(B) Toeprinting assay to examine ribosome binding in the presence and absence of $fMet^{tRNA}$ and $MnCl_2$.

(C) β-galactosidase activity for strains carrying P_{LlacO}-5′UTR_{mntP}-*lacZ* translational fusions with mutations of potential base pairing region highlighted in yellow in (A).

(D) β-galactosidase activity for strains carrying P_{LlacO}-5′UTR_{mntP}-*lacZ* translational fusions with mutations of potential base pairing region highlighted in orange in (A). For β-galactosidase assays in (C-D), cells grown in M9 glucose medium were incubated with or without 400 μM $MnCl_2$ for 1 h, and the results are given in Miller units as the mean ± SDM of three independent samples.

(E) Lead probing of the *mntP* 5′-UTR structure. Filled circles indicate bands that increase for wild type but not mutant *mntP* in the presence of $MnCl_2$, and open circles indicate those bands that decrease. Lanes labeled T1 and OH are the nucleotide size markers derived from the same labeled *mntP* RNA after incubation with RNase T1 or hydroxyl anions, respectively. Nucleotide positions relative to the transcription start site are labeled to the left of the gel. See also Figure S4.

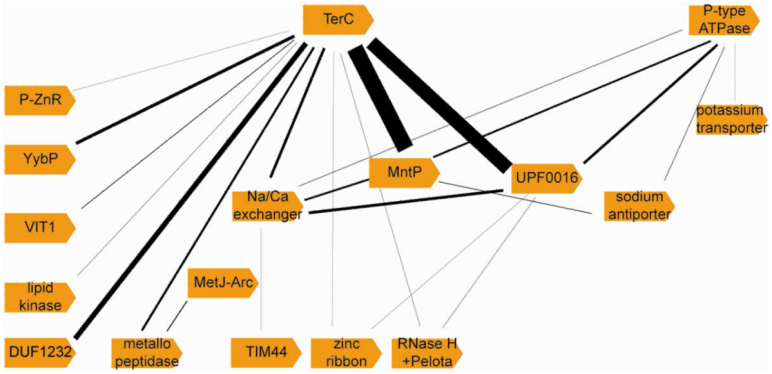

Figure 6. Network of genes immediately downstream of the *yybP-ykoY* riboswitch are predicted to have roles in protecting against metal toxicity

The thickness of the edge (black) connecting genes co-occurring in the same genome downstream of a paralogous *yybP-ykoY* motif is scaled as per the frequency of such a co-occurrence in our dataset (see Table S2). P-ZnR denotes proteins with a peptidase-associated zinc-ribbon and MetJ-Arc denotes proteins with MetJ-Arc DNA-binding domains. Figure S5 is an expanded version of this figure, which includes other genes encoded in the operons along with the genes preceded by *yybP-ykoY* motifs.

Table 1

mntP aptamer binding to $MnCl_2$ during equilibrium dialysis

	μM manganese		
Nucleic acid	**Buffer side**	**Nucleic acid side**	**Percent enrichment**
wild type *mntP* RNA	1.2 ± 0.05	29.4 ± 0.7	96%
$C_{49}A_{50}$ to $A_{49}U_{50}$ mutant RNA	8.0 ± 0.5	21.6 ± 0.6	73%
DNA template	12.3 ± 0.1	17.4 ± 0.7	59%